

# Modeling of C-SNARF-1 pH Fluorescence Properties: Towards Calibration Free Optical Fiber pH Sensing for in Vivo Applications

Rutjaphan Kateklum<sup>1</sup>, Bernard Gauthier-Manuel<sup>1</sup>, Christian Pieralli<sup>1</sup>,  
Samlee Mankhetkorn<sup>2</sup> and Bruno Wacogne<sup>1,3</sup>

<sup>1</sup>FEMTO-ST Institute, Univ. Bourgogne Franche-Comté, CNRS, 25030 Besançon cedex, France

<sup>2</sup>Center of Excellence in Molecular Imaging, Chiang Mai University, 50200 Chiang Mai, Thailand

<sup>3</sup>INSERM CIT1431, Besançon University Hospital, 25000 Besançon, France

**Keywords:** *in Vivo* pH Sensing, Fluorescence, Optical Fiber, pH Sensor, Modelling, Calibration Free Measurement.

**Abstract:** Organic functions of the human body are related to biological constants. Variations of these constants, among them pH, induce pathological troubles. The general goal of our work is to fabricate a fluorescent pH sensor at the end of an optical fiber for *in vivo* pH measurements. One difficulty using fluorescence indicators is the need to perform an accurate calibration. In this communication, we present methods used to simplify and potentially avoid calibration procedures of fluorescence indicators. The first method concerns the simplification of calibration procedures making them independent of the indicator's concentration, path length and equipment used. The second method concerns modelling the fluorescence emission of the molecules as a function of pH only. This model is used to fit the exact shape of C-SNARF-1 fluorescence spectra obtained at any pH. Subsequently, the pH of a solution can be computed with an accuracy of 0.1 pH unit without the calibration procedure employed up to now. These methods constitute the first steps toward calibration free pH measurements. They can be applied to any fluorescent indicator exhibiting a dual emission peak. As a conclusion, this is the first time that fluorescence properties of C-SNARF-1 are fully mathematically described.

## 1 INTRODUCTION

In living beings, biological functions are related to either acid or alkaline constants. Indeed, the action of a protein depends on the surrounding pH. An inadequate value of the pH makes the proteins non active which is deleterious for the organism. A lot of pathologies induce or are the consequence of pH dysregulation. There exist a need for pH sensors which can be used in the human body. Among the wide range of technologies potentially useful for this application, fiber optic fluorescence pH sensing is a promising technique for *in vivo* measurements. The general goal of our work is depicted in figure 1.

Ideally, such a pH sensor should be used in a calibration free manner. For this, the pH sensitive molecules to be grafted at the end of the optical fiber should be chosen with great care. They must exhibit

fluorescence properties which can potentially lead to the desired calibration free measurement.

In this communication, we present the part of the pH sensor's development devoted to this issue.

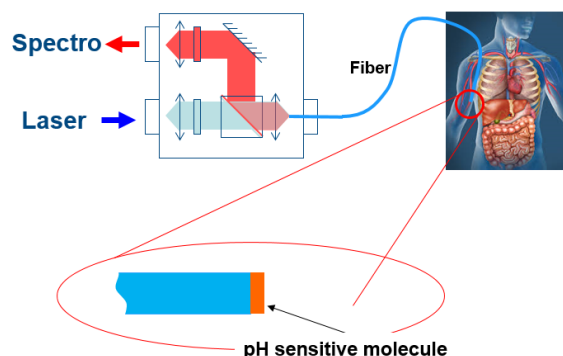


Figure 1: Schematic diagram of the fiber optic pH sensor under development.

Fluorescent indicators can be divided in three main classes (Valeur, 2001). These classes depend whether or not molecules undergo photoinduced proton or electron transfer, or none of them. C-SNARF-1 (5-(and-6)-Carboxy SNARF®-1) belongs to this last class. When in solution, this indicator exists under two forms: the acidic (or protonated) form and the basic (or deprotonated) form. The acid-base reaction equilibrium is driven by the law of mass action.

C-SNARF-1 exhibits a  $pK_a$  equal to 7.5 which makes it a good candidate for sensing in the physiological pH range. As previously mentioned, this indicator exhibits only two forms. Therefore, the fluorescence signal is due to the contribution of these two forms with relative contributions depending on the pH of the solution under test. Each protonated or deprotonated form exhibits characteristic fluorescence and/or absorption spectra (Yassine, 1997). Shifts between spectra obtained for protonated and deprotonated species can be exploited in order to perform a ratiometric measurement. In this case, pH is directly related to the ratio of the fluorescence intensities measured at 2 wavelengths which are characteristic of the indicator used.

However, the reality is a bit more complicated because a calibration of the molecules in solution must be performed. Indeed, pH is related to the activity of  $H^+$  ions and not their concentration. This makes pH determination dependent on factors like ionic strength, specific interactions depending on the chemical nature of the indicator and the surrounding medium as well as structural changes of the medium (Valeur, 2001). Calibration procedure will be described in section 2 together with the method we propose to considerably simplify the procedure.

Note that, to the best of our knowledge, no simplification of the calibration has been proposed to date, except a proposition to perform *in situ* calibration using nigericin (Negulescu, 1990). However, this method may not be applicable in all situations.

In this communication, we also propose a method which potentially can lead to a calibration free pH measurement. This method is based on a mathematical description of the emitted fluorescence spectra as it will be exposed in section 3. Some authors developed mathematical models in order to account for different difficulties encountered in specific applications. For example in (Zurawik, 2016), authors developed a model to account for the small number of free  $H^+$  ions in the yeast mitochondria. In reference (Bottenus, 2009) authors study the pH behavior in nanochannels. In this case,

the  $\zeta$  potential is responsible for charges reorganizations in the channels. In this case however, fluorescence properties of C-SNARF-1 are described in a “law of mass action” approach.

Some authors proposed a more mathematical description of fluorescence properties. In (Ribou, 2002) for example, authors propose to extend the two wavelength ratiometric method to the analysis of the whole fluorescence spectrum. Their approach consists in recording the spectra of both fully protonated and fully deprotonated forms of SNARF. These two extreme pH spectra form a basis which is now used to fit a spectrum recorded at an unknown pH.

In reference (Owen, 1992 (1 and 2)) authors employ the same method based on fitting an unknown spectrum with spectra measured at extreme pHs. The motivation is that ratiometric measurements are based on measuring ratios at two distinct wavelengths with known solutions in order to compute the ratio at unknown pH with values obtained at two measurement wavelengths. In other words, they explain that using two equations to solve two unknowns does not allow accounting for other phenomena which can jeopardize the pH measurement.

Surprisingly, it should be noted that, except work presented in (Zurawik, 2016; Bottenus, 2009), pH measurement difficulties have poorly been addressed recently, despite the availability of compact spectrometers and powerful calculation software which makes mathematical treatment of spectra easy.

In what follows, section 2 is devoted to a new method which considerably simplifies the calibration procedure while section 3 deals with first steps towards calibration measurements. Then, a conclusion will be proposed in section 4.

## 2 SIMPLIFYING CALIBRATION PROCEDURES

Here, we mathematically express the evolution of the emitted energy as a function of pH and excitation wavelengths. This expression can be used to post-process spectra which substantially simplify calibration procedures.

### 2.1 About the Current Calibration Procedure

As previously mentioned, C-SNARF-1 is a pH indicator exhibiting a dual emission peak. This is

illustrated in figure 2. pH can be deduced from the intensity ratio at wavelengths corresponding the maxima emission of both protonated and deprotonated forms.

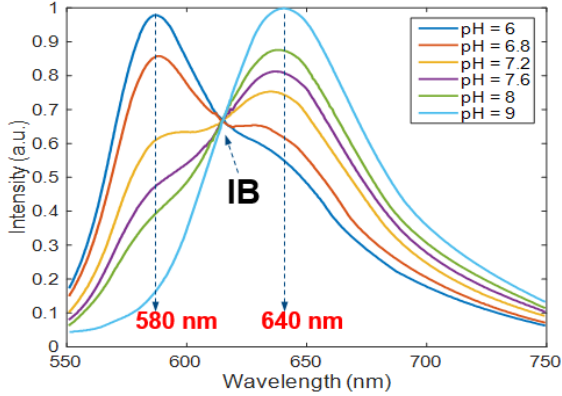


Figure 2: pH dependency of C-SNARF-1 molecules (Thermofisher, no year).

The two wavelengths used for this so-called ratiometric measurement are 580 nm and 640 nm for this molecule. However, measuring the fluorescence emission ratio at two distinct wavelengths does not lead to an exact determination of pH. Indeed, the indicator must be calibrated using two extreme pH solutions for which ratios at measurement wavelengths are calculated. The calibration procedure can be found either in the manufacturer website (Thermofisher, no year) or in various publications (Whitaker, 1991; Ribou, 2002; Graber, 1986; Bancel, 1990). This is illustrated in equation (1). Values of  $R$  and  $I$  coefficients can be found in (Thermofisher, no year). They represent intensity ratios at specific wavelengths.

$$pH = pK_a - \log_{10} \left[ \frac{R - R_B}{R_A - R} \times \frac{I_B^2}{I_A^2} \right] \quad (1)$$

Calibration requires extreme care when performing measurements as explained in (Gryniewicz, 1985) in the case of calcium detection. Adapted from this reference: “any intervening loss of dye or changes in instrument sensitivity jeopardizes the calibration and may be mistaken for a change in  $[H^+]$ ”.

## 2.2 About the Difficulty to Perform Calibrations

When extreme care is not taken, spectra obtained with calibration solutions undergo variations of their intensities. The isosbestic point (IB in figure 2) no longer exists and calibration becomes impossible.

This is illustrated in figure 3 where spectra recorded using basic equipment were obtained. They were recorded using basic plastic cuvette manually placed in front of a fluorescence beam-splitter. Therefore, path-length and multiple reflections in the plastic cuvette were not controlled, maxima of the spectra were randomly distributed, and no isosbestic points was observed.

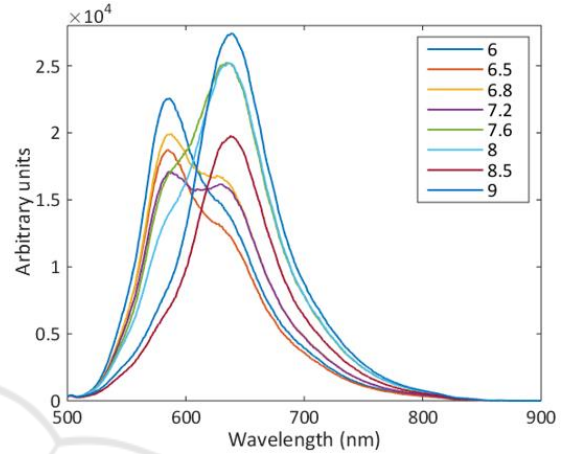


Figure 3: Spectra obtained using basic equipment.

## 2.3 Simplifying the Calibration Procedure

The method we propose is based on the fact that the emission fluorescence energy does not only depend on pH but also on the excitation wavelength. By energy, we understand the integral of the fluorescence spectra.

Here, we mathematically express the evolution of the emitted energy with pH and excitation wavelengths. This equation can now be used to post-process spectra like those presented in figure 3, recalculate the energy they should exhibit and retrieve the existence of the isosbestic point.

Looking at emission spectra for 2 excitation wavelengths given by the supplier (figure 4) (Thermofisher, no year), variations of the energies with pH and excitation wavelength are clearly visible. In fact, 3 excitation wavelengths are available from (Thermofisher, no year) but only 2 sets of spectra are shown for clarity. In the mathematical development presented below, the 3 excitation wavelengths are taken into account.

To describe the evolution of the energies with pH, we must consider contributions of the protonated and deprotonated forms. For an excitation wavelength  $\lambda_{ex}$  at  $pHi$ , the energy can be written as follows.

$$E_{\lambda_{ex}}^{pHi} = [A^-]E_{\lambda_{ex}}^{[A^-]} + [AH]E_{\lambda_{ex}}^{[AH]} \quad (2)$$

In equation (2),  $[A^-]$  and  $[AH]$  represent the concentration in deprotonated and protonated forms respectively,  $E_{\lambda_{ex}}^{[A^-]}$  and  $E_{\lambda_{ex}}^{[AH]}$  represent the energy emitted by the deprotonated and protonated forms respectively.

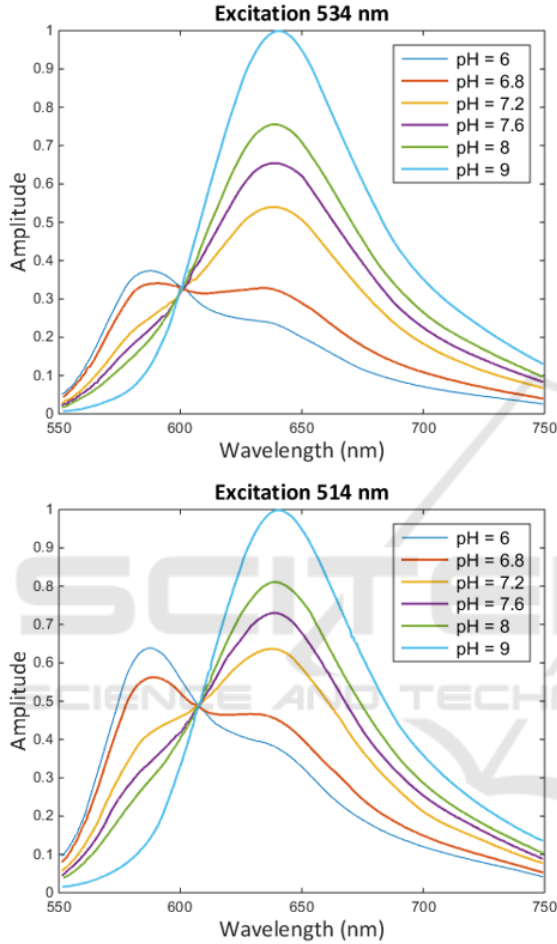


Figure 4: Spectra from supplier for 2 excitation wavelengths (Thermofisher, no year).

It is often interesting to express concentrations in terms of dissociation degree of the molecules. The dissociation degree allows describing proportions in the protonated or deprotonated form from the total concentration in indicator as follows. If we note  $\alpha$  the dissociation degree and  $c_T$  the total indicator's concentration we have:

$$[A^-] = \alpha[SNARF] = \alpha c_T \quad (3)$$

$$[AH] = (1 - \alpha)[SNARF] = (1 - \alpha)c_T \quad (4)$$

The dissociation degree  $\alpha$  is given by:

$$\alpha = \frac{1}{1 + 10^{(pK_a - pH)}} \quad (5)$$

Mixing equations (2) to (5) leads to the evolution of the energies as a function of pH (through the dissociation degree).

$$E_{\lambda_{ex}}^{pHi} = c_T E_{\lambda_{ex}}^{[AH]} + c_T (E_{\lambda_{ex}}^{[A^-]} - E_{\lambda_{ex}}^{[AH]}) \alpha \quad (6)$$

From equation (6), it is clear that the energies evolve according to sigmoid functions. Plotting the emitted energies as a function of pH for the 3 excitation wavelengths and fitting them with equation (6) leads to figure 5. In this figure we recall the expressions of the asymptotic values.

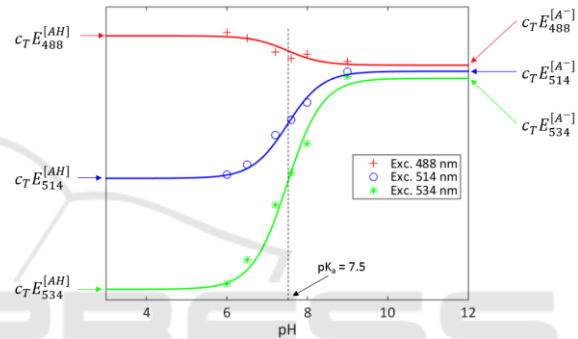


Figure 5: Evolution of the emitted energies as a function of pH and excitation wavelengths.

In the physiological pH range (between 6.5 and 8), the evolution of the energies can be considered linear. The slopes and the intercept of linear parts of curves presented in figure 5 also evolve linearly as shown in figure 6. Therefore, we can define the equation which gives the emitted energy for any pH and any excitation wavelength.

$$f(pH, \lambda_{ex}) = \alpha_2 \cdot pH + \beta_1 \cdot \lambda_{ex} + \alpha_1 \cdot pH \cdot \lambda_{ex} + \beta_2 \quad (7)$$

In equation (7),  $\alpha$  and  $\beta$  coefficients correspond to the linear equation giving the slope and the intercept of linear regions of curves in figure 5 as a function of the excitation wavelength calculated from spectra shown in figure 2.

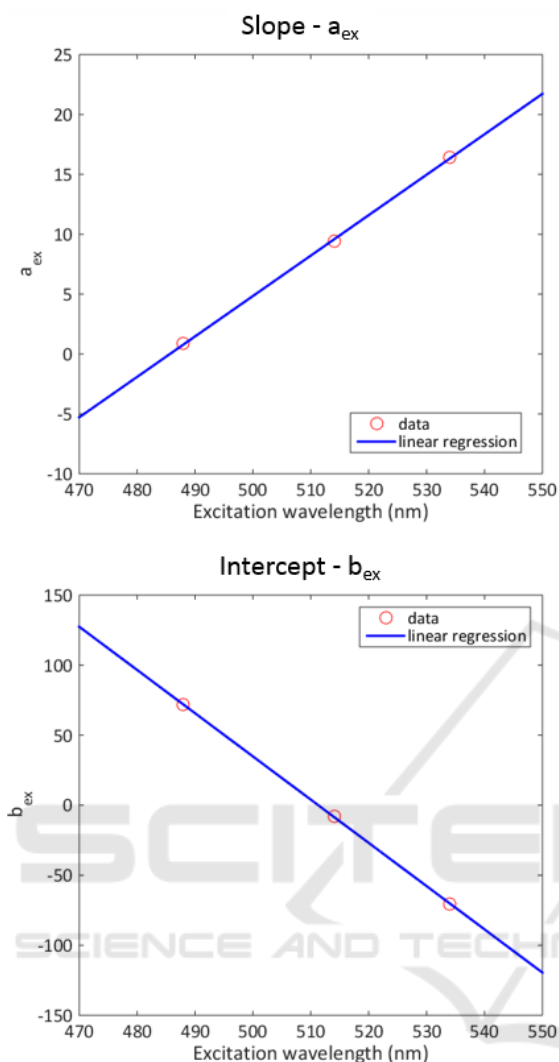


Figure 6: Slope and intercept of the energies as a function of excitation wavelength.

Spectra post-processing is now extremely simple. It consists in 2 main steps. First, spectra recorded at known pH and known excitation wavelength are normalized. Second, normalized spectra are multiplied by equation (2) which gives them the energy they should have (in fact proportionally to each other's). Iterating the process for all pH values allows re-calculating the correct spectra and retrieving the isosbestic point. This is illustrated in figure 7 where spectra of figure 3 have been post-processed.

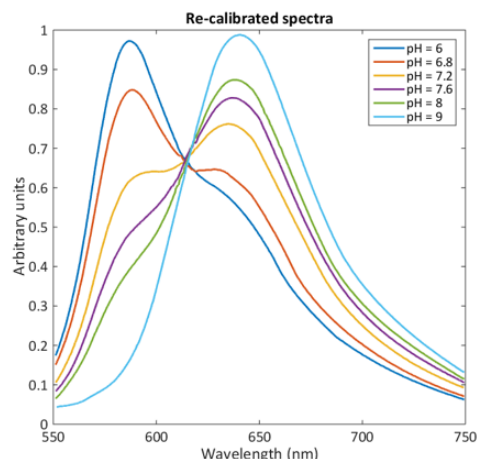


Figure 7: Spectra of figure 3 post-processed with our method.

Note that the calibration procedure only implies ratios of intensities at specific wavelengths. Therefore, losing the energy value of the initial spectra when post-processing them is not an issue.

To summarize, this post-processing considerably simplifies indicators calibration procedures as calibration becomes independent of the indicator's concentration and path length and is not equipment dependent anymore. This method can easily be transposed to other ratiometric pH indicators exhibiting a dual emission peak and also more generally to ion sensing fluorescent indicators exhibiting dual emission peaks and for which the same initial calibration procedure is recommended.

In the next section, we show that we can go a bit further.

### 3 TOWARDS CALIBRATION FREE PH MEASUREMENT

In this section, we show that we can go beyond a simple simplification of calibration procedures. The idea is not to describe spectra at unknown pH using spectra corresponding to the protonated or deprotonated forms of the indicator as previously proposed by different teams and mentioned in the introduction of this communication.

The general goal of the method consists in proposing a full mathematical description of the pH dependency of C-SNARF-1 fluorescence emission. In this way, a complete  $SNARF(\lambda, pH)$  function is defined and can be used to fit spectra obtained at any pH and to compute the actual pH value. For this,

spectra obtained from the supplier are digitalized and processed as follows.

### 3.1 Fitting Spectra with Voigt Functions

For each of the 6 pH values proposed by the supplier, we try to fit the spectra with a sum of “n” Voigt functions. Each individual spectrum is then decomposed in “n” bands. The goal is to find the minimum number of bands required to fully describe spectra. Voigt functions are commonly used in spectroscopy. We also noted that fitting spectra in the wavenumbers domain requires less functions than fitting them in the wavelengths domain. Therefore, in order to present equations with the traditional unit used in fluorescence (nm), the Voigt function associated to the band number  $i$  is written as follows.

$$V_i(\lambda) = A_i \text{Voigt} \left[ 10^7 \left( \frac{1}{\lambda} - \frac{1}{X_i} \right), \sigma_i, \gamma_i \right] \quad (8)$$

In this equation,  $A_i$  represents the area of band  $i$  and  $X_i$  the wavelength corresponding to the center of band  $i$ .  $\sigma_i$  and  $\gamma_i$  represent the half-widths of the Gaussian and Lorentzian profiles respectively. Therefore, a Voigt function is described with 4 parameters.

After some series of fittings, we found out that using 3 functions is enough to fully describe the evolution of the emitted spectrum as a function of the pH. Fitting the spectra from supplier was made using the Levenberg-Marquard algorithm in a multi-branch fitting which includes all spectra obtained with all pH values. We recall that we have 4 parameters per Voigt profile, 3 profiles per pH and 6 pHs available from the supplier’s website. Therefore, 72 parameters are required to fully describe the pH behavior of C-SNARF-1 molecules.

Mathematical developments would be too long to be exposed here but we described each parameter as a function of the dissociation degree  $\alpha$ . In other words, although a large number of parameters are required, only one variable is necessary to fully describe the pH behavior of C-SNARF-1 molecules.

Working on these first series of fittings, we then established a  $SNARF(\lambda, pH)$  function given in equation (9).

$$SNARF(\lambda, pH) = \sum_{i=1}^3 V_i(\lambda) \quad (9)$$

In equation (9), functions  $V_i(\lambda)$  are given by equation (8). The pH dependency of the  $SNARF(\lambda, pH)$  function is included in the  $\alpha$  dependence of the above mentioned parameters.

Figure 8 shows an example of spectrum fitting using 3 Voigt profiles.

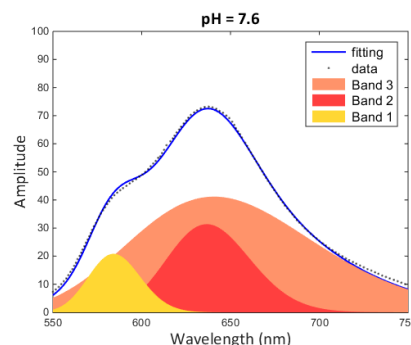


Figure 8: Fitting supplier’s data with 3 Voigt profiles.

Figure 9 shows the evolution of the 3 bands as a function of pH and wavelength.

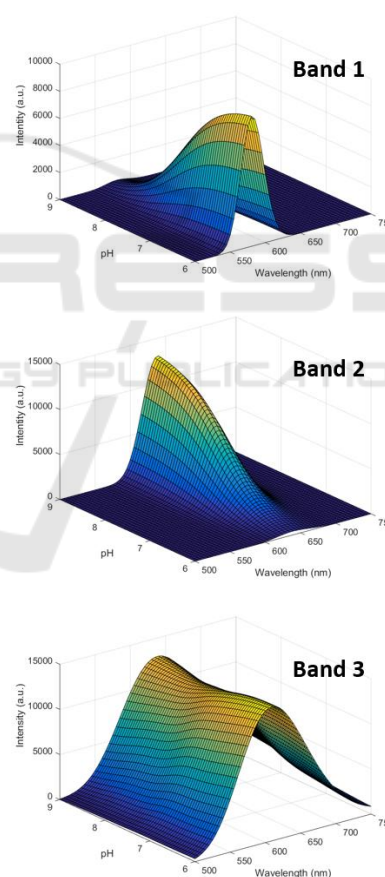


Figure 9: Evolution of the 3 bands as a function of pH and wavelength.

### 3.2 Fitting Any Spectrum with the $SNARF(\lambda, pH)$ Function

The above defined  $SNARF(\lambda, pH)$  function was used to fit uncalibrated spectra presented in figure 3. The goal was to fit these spectra with the  $SNARF(\lambda, pH)$  function in order to compute the value of the pH directly from the shape of the spectra. The result is given in figure 10 for a few pH values.

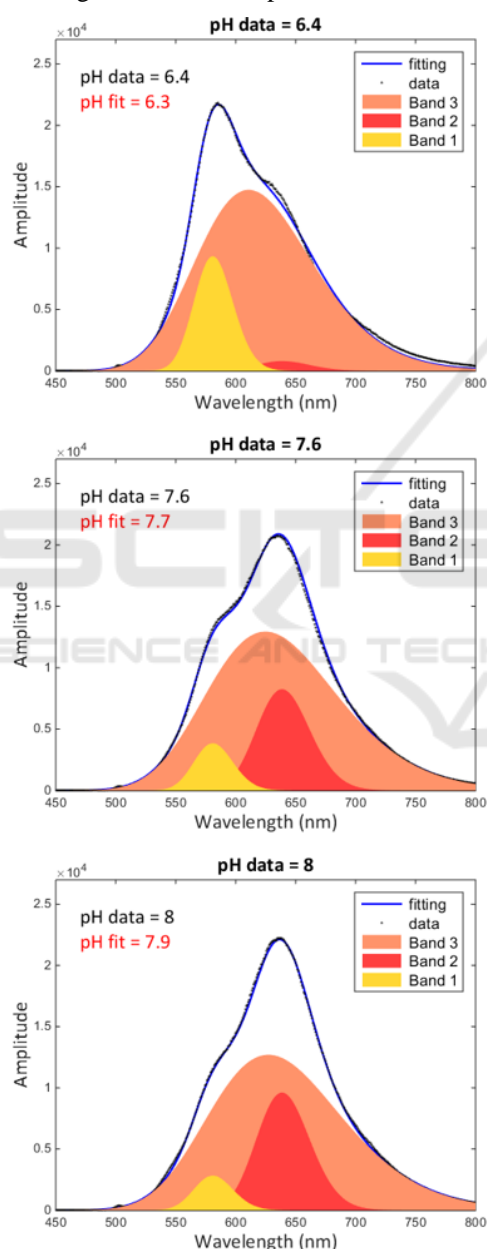


Figure 10: Fitting spectra of figure 2 with the  $SNARF(\lambda, pH)$  function and computing the pH value from the shape of the spectra.

It can be seen that the pH value can be computed with an accuracy of about 0.1 pH unit. This result is particularly encouraging because it was obtained without using any calibration and with spectra measured using non sophisticated equipment. To obtain this, we recall that 72 parameters should be fitted in order to generate the  $SNARF(\lambda, pH)$  function. Although the number of parameters is quite large, fitting remains highly accurate because of the even larger number of experimental data. Indeed, the  $SNARF(\lambda, pH)$  function was determined using spectra presented in figure 2. We have about 1000 data points to describe each of the 6 spectra. This means that 72 parameters are fitted considering about 6000 data points.

Further development must be conducted in order to improve the accuracy of the method. In particular, attention should be paid to the influence of the ionic strength on the value of the  $pK_a$  and possibly on the shape of the emitted spectra. Using the same fitting method to account for possible changes of the shape of the spectra due to variations in the ionic strength should allow improving the accuracy of the method and possibly demonstrate the first calibration free pH measurement.

## 4 CONCLUSIONS

In this communication, we have presented methods used to considerably simplify calibration procedures applied to dual wavelengths ionic fluorescent indicators and potentially employed to progress towards calibration free measurements. For demonstration purpose, we presented results obtained with C-SNARF-1 molecules when performing a fluorescence pH sensing.

Simplifying the calibration procedures rely on the expression of the evolution of the emitted energies as a function of pH and excitation wavelengths. This method makes calibration procedures independent of the experimental conditions. A step towards calibration free pH measurement was proposed using a full mathematical description of the pH dependency of C-SNARF-1 molecules. Using the  $SNARF(\lambda, pH)$  function defined using our fitting algorithm allowed computing pH directly from the analysis of the shapes of the emitted spectra without any preliminary calibration. Note that calibration free pH measurement has never been demonstrating regardless the technology used. Taking into account the influence of the ionic strength should further enhance the pH determination accuracy which is 0.1 pH unit in the examples given here.

Molecules like C-SNARF-1 were mainly developed for fluorescence imaging of intra-cellular pH which requires the use of confocal microscope where the analysis of the fluorescence spectrum is not possible. However, there exists multi-channel confocal microscopes which allow obtaining images at different fluorescence wavelengths. Because the model is established, images obtained for a reduced number of individual emission wavelengths may be sufficient to reconstruct the whole spectra shape, hence allowing pH determination without calibration.

Concerning the fabrication of a fluorescent fiber optic pH sensor, work is still ongoing using C-SNARF-1 as a pH indicator. Fiber optic pH measurement based on the analysis of the spectra shapes should be presented shortly.

## ACKNOWLEDGEMENTS

This work was partially supported by the European Commission [grant number FE2007/2013, operation 36381].

## REFERENCES

<https://www.thermofisher.com/fr/fr/home/references/molecular-probes-the-handbook/ph-indicators/probes-useful-at-near-neutral-ph.html>.

Bancel, F., Vigo, J., Salmon, J.M. and Viallet, P., 1990, Acid—base and calcium-binding properties of the fluorescent calcium indicator indo-1, *Journal of Photochemistry and Photobiology A: Chemistry*, 53, pp. 397-409.

Bottenus, D., Oh, Y.J., Sang M. Han, Cornelius and Ivory, F., 2009, *Experimentally and theoretically observed native pH shifts in a nanochannel array*, *Lab Chip*, Vol. 9, pp. 219-231.

Graber, M.L., DiLillo, D.C., Friedman, B.L. and Pastoriza-Munoz, E., 1986, *Characteristics of fluoroprobes for measuring intracellular pH*, *Analytical Biochemistry*, Vol. 156, pp. 202-212.

Grynkiewicz, G., Poenie, M., and Tsien, R.Y., 1985, A new generation of Ca<sup>2+</sup> indicators with greatly improved fluorescence properties, *Journal of biological chemistry*, Vol. 260, pp. 3440-3450.

Negulescu, P.A. and Machen, T.E., 1990, *Intracellular ion activities and membrane transport in parietal cells measured with fluorescent dyes*, *Methods Enzymol.*, Vol.192, pp. 38-81.

Owen, C.S., 1992, *Comparison of spectrum-shifting intracellular pH probes 5'(and 6')-carboxy-10-dimethylamino-3-hydroxyspiro[7H-benzo[c]xanthene-7, 1'(3'H)-isobenzofuran]-3'-one and 2',7'*

*biscarboxyethyl-5'(and 6')-carboxyfluorescein*, *Analytical Biochemistry*, Volume 204, pp. 65-71.

Owen, C.S., Carango, P., Grammer, S., Bobyock, S., Leeper, D.B., 1992, pH-dependent intracellular quenching of the indicator carboxy-SNARF-1, *Journal of fluorescence*, Vol. 2, pp. 75-80.

Ribou, A.C., Vigo, J., and Salmon, J.M., 2002, C-SNARF-1 as a fluorescent probe for pH measurements in living cells: two-wavelength-ratio method versus whole-spectral-resolution method, *J. of Chem. Educ.*, Vol. 79, pp. 1471-1474.

Valeur, B., 2001, *Molecular Fluorescence: Principles and Applications*. 2001 Wiley-VCH Verlag GmbH. ISBNs: 3-527-29919-X (Hardcover); 3-527-60024-8 (Electronic).

Whitaker, J.E., Haugland, R.P., and Prendergast, F.G., 1991, *Spectral and photophysical studies of benzo[c]xanthene dyes: Dual emission pH sensors*, *Analytical Biochemistry*, Volume 194, pp. 330-344.

Yassine, M., Salmon, J.M., Vigoand, J. and Viallet, P., 1997, C-SNARF-1 as a pHi fluoroprobe: discrepancies between conventional and intracellular data do not result from protein interactions”, *Journal of Photochemistry and Photobiology B: Biology*, Vol. 37, pp. 18-25.

Żurawik, T.M., Pomorski, A., Belczyk Ciesielska, A., Goch, G., Niedźwiedzka, K., Kucharczyk, R., Krezel, A. and Bal, W., 2016, *Revisiting Mitochondrial pH with an Improved Algorithm for Calibration of the Ratiometric 5(6)-carboxy-SNARF-1 Probe Reveals Anticooperative Reaction with H+ Ions and Warrants Further Studies of Organellar pH*, PLoS ONE 11: e0161353.